

B Cell Translocation Gene 2 Enhances Susceptibility of HeLa Cells to Doxorubicin-induced Oxidative Damage*

Received for publication, June 3, 2008, and in revised form, October 7, 2008. Published, JBC Papers in Press, October 7, 2008, DOI 10.1074/jbc.M804255200

Young-Bin Lim, Tae Jun Park, and In Kyoung Lim¹

From the Department of Biochemistry and Molecular Biology, Ajou University School of Medicine, Suwon, 443-721, Korea

BTG2^{TIS21/PC3} (B cell translocation gene 2) has been known as a p53 target gene and functions as a tumor suppressor in carcinogenesis of thymus, prostate, kidney, and liver. Although it has been known that the expression of BTG2^{TIS21/PC3} is induced during chemotherapy-mediated apoptosis in cancer cells, a role of BTG2^{TIS21/PC3} in cell death remains to be elucidated. In this study, the mechanism and role of BTG2 involved in the enhancement of doxorubicin (DOXO)-induced cell death were examined. Treatment of HeLa cells with DOXO revealed apoptotic phenomena, such as chromatin condensation and cleavage of poly(ADP-ribose) polymerase and lamin A/C with concomitant increase of BTG2^{TIS21/PC3} expression. Employing infections of Ad-TIS21 virus and lentivirus with short hairpin RNA to BTG2, the effect of BTG2^{TIS21/PC3} on the DOXO-induced apoptosis of HeLa cells and liver cancer cells was evaluated. Not only short hairpin RNA-BTG2 but also *N*-acetyl-L-cysteine significantly reduced the DOXO-induced HeLa cell death and generation of H₂O₂. Moreover, forced expression of BTG2^{TIS21/PC3} using adenoviral vector augmented DOXO-induced cancer cell death concomitantly with increase of manganese-superoxide dismutase but not catalase, CuZnSOD, and glutathione peroxidase 1. The increased apoptosis by forced expression of BTG2^{TIS21/PC3} could be inhibited by *N*-acetyl-L-cysteine and polyethylene glycol-catalase. These results therefore suggest that BTG2^{TIS21/PC3} works as an enhancer of DOXO-induced cell death via accumulation of H₂O₂ by up-regulating manganese-superoxide dismutase without any other antioxidant enzymes. In summary, BTG2^{TIS21/PC3} enhances cancer cell death by accumulating H₂O₂ via imbalance of the antioxidant enzymes in response to chemotherapy.

TIS21 (12-*O*-tetradecanoylphorbol-13-acetate-inducible sequence 21) was first identified as one of immediate early genes (1) in mice 3T3 fibroblasts when treated with 12-*O*-tetradecanoylphorbol-13-acetate (2). Since then, PC3 (pheochromocytoma cell 3) was isolated as an immediate early response gene when activated by nerve growth factor at the onset of neuronal differentiation in rat PC12 cells (3). The human hom-

olog of TIS21, named BTG2 (B cell translocation gene 2), was cloned from a cDNA library of human lymphoblastoid cells as a gene associated with DNA damage response and contains p53 response elements in its 5'-flanking (-74 to -112) region (4).

We previously reported that TIS21 expression was low in thymic carcinoma developed in the SV40 large T antigen transgenic mice but high in normal thymus, suggesting anticarcinogenic activity of TIS21 in thymus (5). Expressions of TIS21 in renal proximal tubule and prostate acini are lost also in the renal carcinoma and the early stage of carcinogenesis in prostate (6, 7), respectively. Consistent with these findings, Boiko *et al.* (8) recently ascertained BTG2 as a tumor suppressor by showing that BTG2 is a major downstream effector of p53-dependent proliferation arrest of mouse and human fibroblasts transduced with oncogenic Ras and that repression of BTG2 regulates the activities of cyclin D1 and cyclin E and phosphorylation of pRB, thus inducing neoplastic transformation of primary human fibroblasts. TIS21 has been known to work also independently of pRB and p53 in cancer cells regulating G₁/S arrest and G₂/M arrest by inhibiting synthesis of cyclin E and cdk4 (9), as well as interaction with cyclin B1 and the cdk1 complex (10), respectively. Moreover, persistent expression of TIS21 induces the loss of mitochondrial membrane potential differences in U937 cells (11), and transfection of TIS21 gene to Huh7 hepatoma cells significantly reduces *in vivo* and *in vitro* tumorigenesis by inhibiting feedback regulation between cyclin B1 and FoxM1 transcription factor (11), and the expression of BTG2 in human liver cancer is much lower than that of the surrounding tissues. Collectively, these findings indicate that TIS21 controls cellular process as an inhibitor of cell division cycle and a tumor suppressor, thus evading cancer development independent of p53.

The level of reactive oxygen species (ROS)² is controlled by multiple interacting components. Among them, superoxide dismutase (SOD), glutathione peroxidase 1 (GPx), and catalase are the primary antioxidant enzymes in mammalian tissues (12, 13). SOD catalyzes dismutation of superoxide anion to hydrogen peroxide, which is further detoxified by catalase and GPx. In mammals, there are at least three forms of SOD: cytosolic CuZnSOD, extracellular ECSOD, and mitochondrial MnSOD. MnSOD knock-out mice die within 18 days after birth, suggesting

* This work was supported by Research Grants R01-2006-000-10311-0 and M10756040001-07N5604-00110 from the Korea Science and Engineering Foundation. The costs of publication of this article were defrayed in part by the payment of page charges. This article must therefore be hereby marked "advertisement" in accordance with 18 U.S.C. Section 1734 solely to indicate this fact.

¹ To whom correspondence should be addressed: Dept. of Biochemistry and Molecular Biology, Ajou University School of Medicine, Suwon, 443-721, Korea. Tel.: 82-31-219-5051; Fax: 82-31-219-5059; E-mail: iklim@ajou.ac.kr.

² The abbreviations used are: ROS, reactive oxygen species; DOXO, doxorubicin; PARP, poly(ADP-ribose) polymerase; NAC, *N*-acetyl-L-cysteine; MnSOD, manganese-superoxide dismutase; GPx, glutathione peroxidase 1; H₂-DCFDA, 2,2'-dichlorodihydrofluorescein diacetate; PYRO, pyrogallol; shRNA, short hairpin RNA; DMSO, dimethyl sulfoxide; PEG, polyethylene glycol; RT, reverse transcription; HA, hemagglutinin; NBT, nitro blue tetrazolium salt; Ad-β-Gal, adenovirus with bacterial β-galactosidase; m.o.i., multiplicity of infection; MEF, mouse embryonic fibroblast(s).

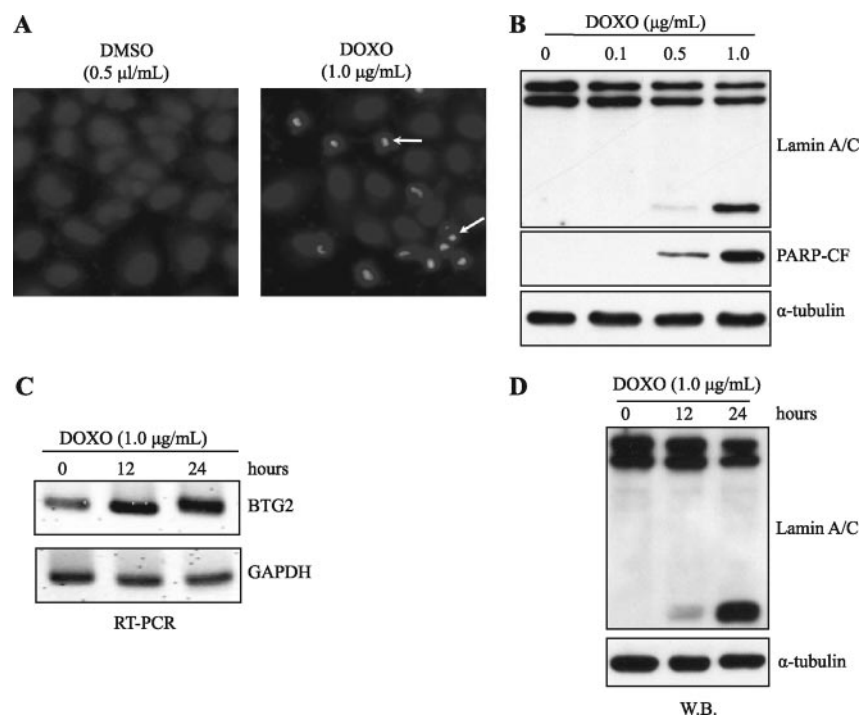


FIGURE 1. **DOXO-induced cell death accompanied with BTG2^{TIS21} expression.** *A*, immunocytochemistry showing chromatin condensation only in the DOXO-treated cells. HeLa cells were treated with either DMSO or DOXO (1.0 $\mu\text{g}/\text{ml}$) for 24 h, and the nuclei were stained with Hoechst dye. *B*, immunoblot analysis revealing degradations of lamin A/C and PARP by DOXO treatment. HeLa cells were treated with indicated concentrations of DOXO for 24 h. Cleavages of PARP and lamin A/C (the substrates of caspase-3 and caspase-7, and caspase-6, respectively) were observed with 0.5 $\mu\text{g}/\text{ml}$ and more of DOXO. α -Tubulin was examined as a loading control. *C*, RT-PCR analysis showing a higher expression of BTG2^{TIS21} mRNA in 12 h of DOXO treatment. HeLa cells were exposed to 1.0 $\mu\text{g}/\text{ml}$ of DOXO for indicated times. *D*, confirmations of time and concentration of DOXO treatment to induce HeLa cell death. HeLa cells were exposed to 1.0 $\mu\text{g}/\text{ml}$ of DOXO for indicated times. Cleavage of lamin A/C was observed after 12 h of DOXO treatment by immunoblot analysis. The data represent typical results from four independent experiments. *W.B.*, Western blot.

that MnSOD is an essential enzyme (14). On the other hand, it is reported that MnSOD has the opposite effect, for instance, overexpression of SOD in *Escherichia coli* results in an increased sensitivity to paraquat and hyperoxia (15), as well as ionizing radiation caused by apparently increased generation of H₂O₂ (16). In addition, overexpression of MnSOD revealed higher sensitivity to ROS in human prostate carcinoma cells (17).

Although it has been known that the expression of BTG2^{TIS21/PC3} is induced during chemotherapy-induced apoptosis in various cancer cells (18–20), the role of BTG2^{TIS21/PC3} in cell death remains to be elucidated. Despite the fact that a large body of studies has consistently suggested that BTG2 functions as a tumor suppressor, BTG2^{-/-} ES cells are more sensitive to DOXO when compared with BTG2^{+/+} ES cells (4). To our best knowledge, there is yet no report regarding how TIS21^{/BTG2} induces the apoptosis of cancer cells in response to chemotherapy. Therefore, we investigated, in the present study, the role of BTG2 in the process of DOXO-induced apoptosis of cancer cells and found that BTG2 enhanced DOXO-induced oxidative damage via imbalance of antioxidant enzymes and worked as a pro-apoptotic gene in the cell death process.

EXPERIMENTAL PROCEDURES

Cell Cultures—HeLa cells were grown in Dulbecco's modified Eagle's medium supplemented with heat-inactivated 10% (v/v) fetal bovine serum in a humidified atmosphere containing

5% CO₂ at 37 °C. The medium was changed every other day. All of the doxorubicin treatments were performed in the culture medium (Dulbecco's modified Eagle's medium) containing 10% (v/v) fetal bovine serum. Immediately before treatment, the medium was removed and replaced with fresh medium.

Reagents—*N*-Acetyl-L-cysteine, PEG-catalase, and pyrogallol were purchased from Sigma-Aldrich. Doxorubicin was from Tocris Bioscience.

Nuclear Staining with Hoechst Dye—Staining was performed as described (21). In brief, control and treated cells (1 $\mu\text{g}/\text{ml}$ doxorubicin for 24 h) were fixed with 3.7% (v/v) paraformaldehyde in phosphate-buffered saline for 10 min at room temperature and permeated with 0.1% Triton X-100 for 10 min at room temperature. The fixed cells were stained with Hoechst 33258 for 5 min, washed, and then examined by fluorescence microscopy (340-nm excitation and 510-nm barrier filter). Apoptotic cells were identified by the presence of highly condensed or fragmented nuclei.

Preparation of Cell Lysates and

Western Blot Analysis—To prepare a total cell lysate, the cells were washed in ice-cold phosphate-buffered saline and lysed in 50 mM Tris, pH 7.4, containing 150 mM NaCl, 1 mM EDTA, 1 mM phenylmethylsulfonyl fluoride, 1 $\mu\text{g}/\text{ml}$ aprotinin, 1 $\mu\text{g}/\text{ml}$ leupeptin, 1 $\mu\text{g}/\text{ml}$ pepstatin, 1 mM NaF, 1 mM sodium orthovanadate, 0.25% sodium deoxycholate, and 1% Nonidet P-40. The supernatants were collected after centrifugation at 10,000 $\times g$ for 10 min. 50- μg aliquots of protein samples were size-fractionated by electrophoresis and then transferred to nitrocellulose membrane. The membranes were immunoblotted with primary antibodies and horseradish peroxidase-conjugated anti-mouse IgG. The immunoblotted proteins were visualized by a chemiluminescence ECL system (Amersham Biosciences). The primary antibodies were purchased from the following sources: anti-lamin A/C and anti-HA from Cell Signaling; anti-PARP from Zymed Laboratories Inc.; anti-MnSOD, anti-GPx, and anti-catalase from Lab Frontier; anti- α -tubulin from Santa Cruz Biotechnology.

Lentiviral shRNA Production and in Vitro Transduction—PLKO.1 lentiviral vectors expressing shRNAs against BTG2 were purchased from Open Biosystems. For BTG2, five preformed constructs were obtained and tested to identify the constructs, which were able to achieve efficient knockdown using RT-PCR. Lentiviral vector stock was produced in 293T cells by transient cotransfection of shRNA construct together with pHR8.2R and pCMV-VSV-G helper constructs using Lipo-

Pro-apoptotic Activity of BTG2 in Doxorubicin-induced Cancer Cell Death

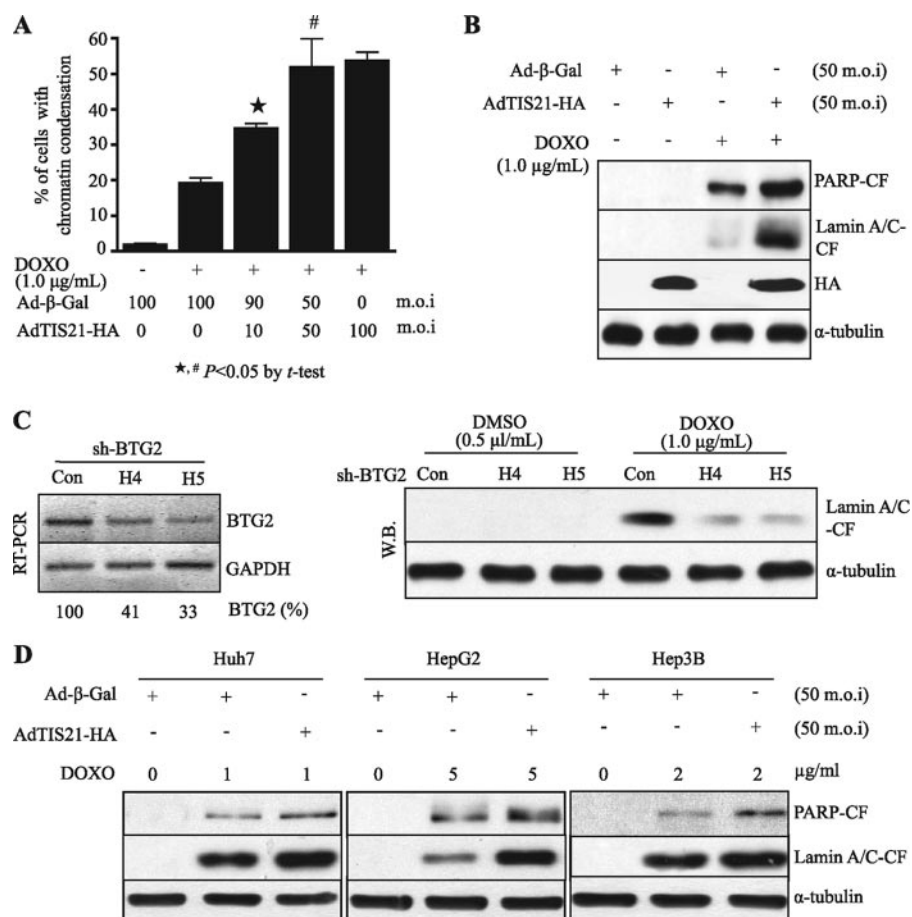


FIGURE 2. BTG2^{TIS21} enhanced DOXO-induced cell death in human cancer cell lines. *A*, increase of chromatin condensation in HeLa cells after treatment with DOXO and Ad-TIS21 virus. HeLa cells were infected with adenoviral vector expressing HA-tagged BTG2^{TIS21} (Ad-TIS21-HA) or β-galactosidase (Ad-β-Gal) for 36 h and then treated with DMSO or DOXO (1.0 μg/ml) for 12 h. Hoechst dye staining was performed, and the cells with chromatin condensation were counted. *, *p* < 0.05 versus DOXO and Ad-β-Gal treated cells; #, *p* < 0.05 versus DOXO and Ad-BTG2^{TIS21} (10 m.o.i.)-treated cells. The data represent the means and standard deviation from four independent experiments. *B*, Western blot analysis showing the increased cleavage of PARP and lamin A/C in HeLa cells after infection with Ad-TIS21 virus (50 m.o.i.) compared with the cells treated with DOXO alone or DMSO for 12 h. Anti-HA shows the level of TIS21 expression. *C*, inhibition of DOXO-induced cell death by lentivirus infection containing short hairpin-BTG2 sequences. HeLa cells were infected either with empty vector (*Con*) or sh-BTG2 virus (*H4* and *H5*), and knockdown of BTG2 expression and the accompanying inhibition of cell death were examined then by RT-PCR and Western blot analyses, respectively. RT-PCR analysis of the level of BTG2 mRNA was normalized to the level of glyceraldehyde-3-phosphate dehydrogenase mRNA, and the level was indicated at the bottom of the data. Note inhibition of BTG2 expression by sh-RNA (*H5*) more than 60%. *D*, enhanced cell death by Ad-TIS21 infection in liver cancer cells. Huh7, HepG2, and Hep3B cells were infected with Ad-TIS21 virus and then treated with either DMSO or DOXO (1.0 μg/ml) for 36 h. The cleavages of PARP and lamin A/C were examined by Western blotting. Note the increase of PARP and lamin A/C cleavages. The data represent a typical result from four independent experiments.

fectamine. The supernatants were harvested after 30 h and filtered through a 0.22-micron filter (Millipore) to remove any nonadherent 293T cells. Next, HeLa cells (5×10^4 in 35-mm-diameter culture dishes) were transduced with 1 ml of virus containing supernatant supplemented with 8 μg of Polybrene. The medium was changed 1 day postinfection, and fresh medium was applied for 2 days.

RT-PCR—Total cellular RNA was prepared by standard TRIzol-based methods. 1 μg of total RNA was reverse-transcribed with oligo(dT) using the Superscript II reverse transcriptase kit (Invitrogen), according to the manufacturer's protocol. RT product (1/50 volume) was applied to PCR. cDNA fragments of BTG2 (175 bp) and glyceraldehyde-3-phosphate dehydrogenase (195 bp) were amplified using the following

primers: sense, 5'-CGAGCAGAG-GCTTAAGGTCTTC-3', and anti-sense, 5'-CTGGCTGAGTCCGAT-CTGG-3' for BTG2; and sense, 5'-CCATGGAGAAGGCTGGGG-3', and antisense, 5'-CAAAGTTGTC-ATGGATGACC-3' for glyceraldehyde-3-phosphate dehydrogenase.

Measurement of Intracellular Hydrogen Peroxide and Superoxide Anion Concentration—The intracellular H₂O₂ concentration was measured by fluorescence-activated cell sorter analysis using 50 μM 2,7-dichlorodihydrofluorescein diacetate (H₂-DCFDA) (D-399; Molecular Probes) in a cell culture system as described (22). In brief, the cells were pretreated with H₂-DCFDA for 10 min prior to cell harvest. H₂O₂ generation was determined with FACScan (BD Biosciences) by measuring the fluorescence of dichlorodihydrofluorescein arising from the oxidation of H₂-DCFDA. Nitro blue tetrazolium salt (NBT) forms a water-insoluble blue formazan when it reacts with intracellular superoxide, showing the degree of superoxide formation within the cell. Chromogenic detection of superoxide was performed using NBT as described (23). In brief, control cells and cells treated with 50 μM pyrogallol for 3 h were incubated with NBT (1.6 mg/ml) in Hanks' balanced salt solution. After a wash in methanol, formazan crystals were extracted with 560 μl of 2 M KOH and 480 μl of DMSO. Absorbance was measured at 575 nm. The results were expressed as A₅₇₅ obtained from 10⁶ cells.

Construction and Use of Adenoviral Vectors—Adenoviral vector expressing TIS21 (Ad-TIS21) was prepared as described (24). In brief, cDNA of TIS21 inserted into replication-defective E1- and E3-adenoviral vectors were transfected and then amplified in 293 human kidney epithelial cells. Adenovirus with bacterial β-galactosidase (Ad-β-Gal) was also prepared for control experiment.

MnSOD Activity Assay—To measure MnSOD activity, cells were collected with a rubber policeman and sonicated in cold 20 mM HEPES buffer, pH 7.2 (EGTA 1 mM, 210 mM mannitol, and 70 mM sucrose), followed by centrifugation at 1,500 × *g* for 5 min at 4 °C. The supernatant was subsequently centrifuged at 10,000 × *g* for 15 min at 4 °C. The resulting pellet was homogenized with HEPES buffer containing 0.1% Triton X-100 and subjected to MnSOD activity assay using a superoxide dis-

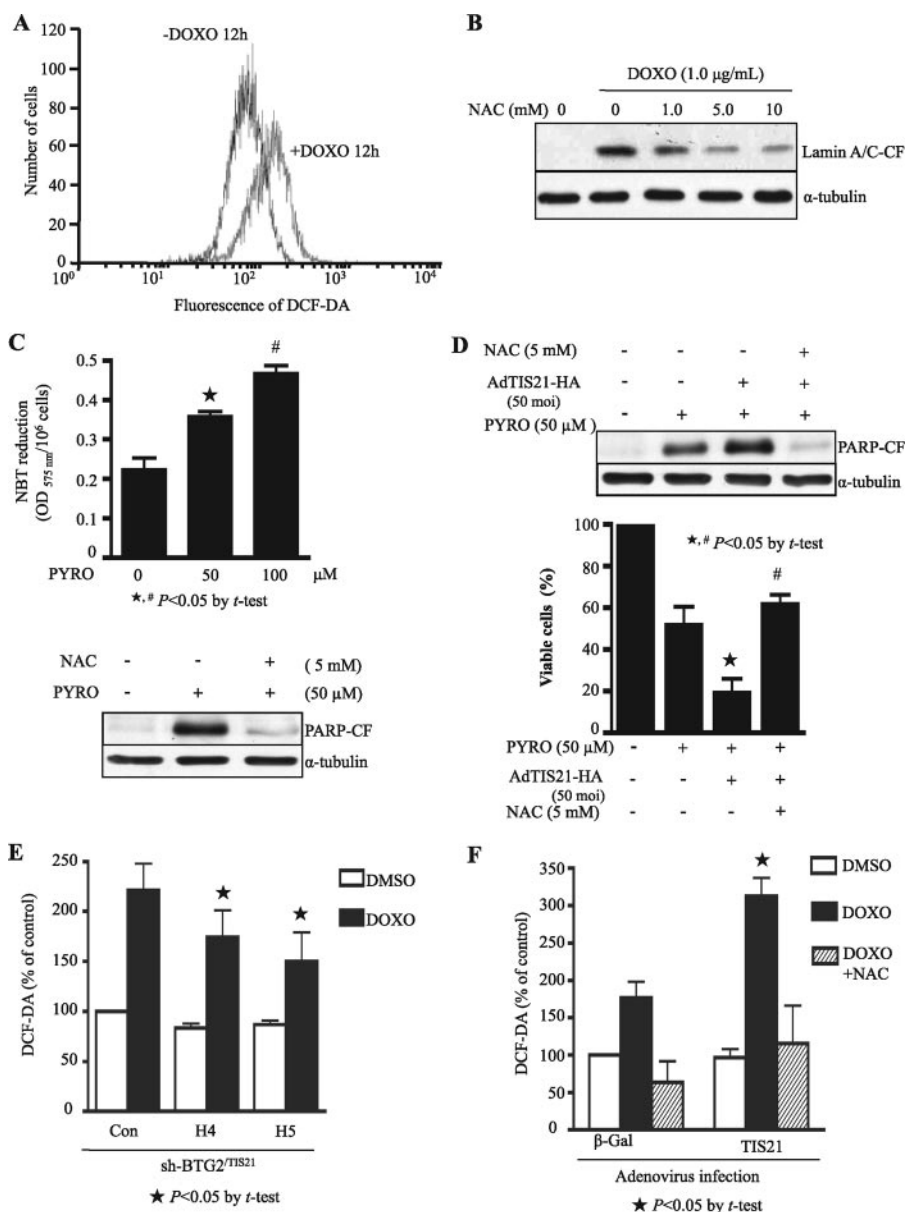


FIGURE 3. BTG2^{TIS21} up-regulated generation of ROS induced by doxorubicin treatment. *A*, fluorescence-activated cell sorter analysis showing DOXO-induced ROS in HeLa cells. The cells were treated with DOXO (1.0 μg/ml) for 12 h, and DCFDA fluorescence generated by ROS was measured by flow cytometry. *B*, Western blot analysis showing the inhibition of DOXO-induced cell death by pretreatment with NAC. HeLa cells were pretreated for 1 h with or without indicated concentrations of NAC and subsequently treated with DOXO (1.0 μg/ml) for 24 h. Note the significant decrease of lamin A/C cleavage by NAC. *C*, inhibition of pyrogallol-induced cell death by NAC. *Upper panel*, HeLa cells were incubated with indicated concentrations of PYRO, superoxide generator, with NBT for 3 h, and NBT reduced by superoxide anion was then examined by measuring the A₅₇₅. *, *p* < 0.05 versus PYRO (0 μM); #, *p* < 0.05 versus PYRO (50 μM). *Lower panel*, HeLa cells were pretreated with either PYRO (50 μM) or NAC (5 mM) for 48 h, and then cleavage of PARP was examined by Western blot analysis. Note the significant inhibition of PYRO-induced cell death by NAC. *D*, TIS21 enhanced PYRO-induced cell death, whereas NAC inhibited cell death. HeLa cells were infected with 50 m.o.i. of Ad-TIS21 or Ad-β-Gal as a control, and then cell death was induced by treatment of the cells with PYRO (50 μM) for 48 h with or without NAC (5 mM) pretreatment. *Upper panel*, Western blotting to determine the cleavage of PARP. *Lower panel*, viable cells were determined by trypan blue staining. The data indicate inhibition of PYRO-induced changes by NAC, suggesting *in vivo* conversion of PYRO-induced superoxide to H₂O₂. *, *p* < 0.05 versus PYRO-treated, Ad-β-Gal-infected; #, *p* < 0.05 versus PYRO-treated Ad-TIS21-infected. *E*, inhibition of DOXO-induced ROS generation by sh-BTG2 RNA. HeLa cells infected with shRNA, H4 and H5, virus, or empty vector (*Con*) were exposed to 1.0 μg/ml of DOXO for 12 h, and DCFDA fluorescence produced by ROS was measured by flow cytometry. *, *p* < 0.05 versus *Con* with DOXO treatment. *F*, enhancement of DOXO-induced ROS generation by Ad-TIS21 infection and efficient inhibition by pretreatment with NAC. HeLa cells were infected with either 50 m.o.i. of Ad-TIS21 or Ad-β-Gal as a control, and then cell death was induced by treatment with either DMSO or DOXO (1.0 μg/ml) for 12 h with or without NAC (5 mM) pretreatment. DCFDA fluorescence produced by ROS was measured by flow cytometry. *, *p* < 0.05 versus DOXO-treated and Ad-β-Gal infected cells. The data represent results of a typical experiment or average values with standard deviations from four independent experiments.

mutase assay kit (SOD-560; Applied Bioanalytical Labs) according to the manufacturer's protocol. The activity of MnSOD was measured in the presence of 2 mM potassium cyanide, an inhibitor of CuZnSOD.

Statistics—The results were expressed as the means ± S.D. from three to four experiments performed independently. Paired Student's *t* test was performed where indicated, and *p* < 0.05 was considered significant.

RESULTS

Doxorubicin-induced Cell Death Accompanied with BTG2^{TIS21} Expression

Doxorubicin is one of the well known chemotherapeutic agents and inducers of apoptosis in various tumor cells including HeLa cells (25). As reported, when HeLa cells were treated with DOXO, chromatin condensation, evidenced by Hoechst dye staining (Fig. 1A), and cleavages of PARP (substrate of caspase-3 and -7) and lamin A/C (substrate of caspase 6) were observed in dose-dependent manner (Fig. 1B). To investigate the possible involvement of BTG2 in DOXO-induced cell death, HeLa cells were exposed to DOXO for 24 h, and the time-dependent cleavage of lamin A/C (Fig. 1D) with a concomitant increase of BTG2 expression were observed in 12 h (Fig. 1C), suggesting that BTG2 may have a role in the process of DOXO-induced cell death.

BTG2^{TIS21} Enhanced DOXO-induced Cell Death in Human Cancer Cell Lines—To examine the role of BTG2 in DOXO-induced cell death, HeLa cells were infected with HA-tagged Ad-TIS21 virus or Ad-β-Gal as the control. Infection of the cells with Ad-TIS21 virus (10–100 m.o.i.) significantly increased the number of cells with chromatin condensation in response to DOXO treatment, as compared with that of the control (Fig. 2A). Based on the data in Fig. 2A, HeLa cells were infected with viruses (50 m.o.i.) and then treated with DOXO, and the expression of TIS21 was examined by Western blot analysis using

Pro-apoptotic Activity of BTG2 in Doxorubicin-induced Cancer Cell Death

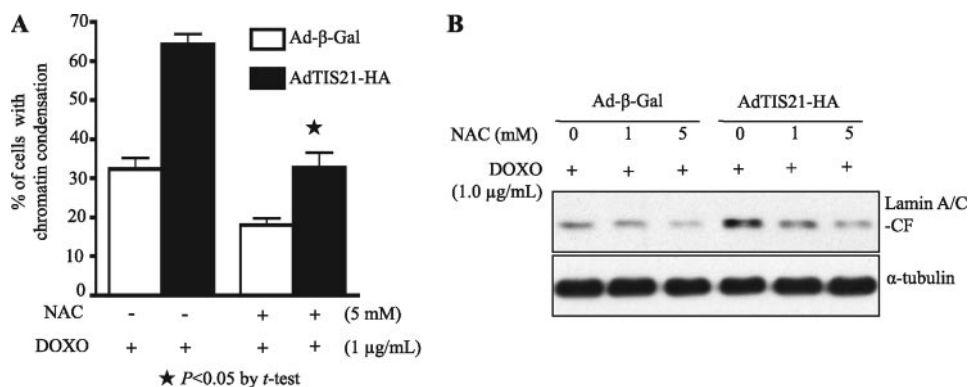


FIGURE 4. NAC abolished the effect of BTG2^{TIS21} on DOXO-induced cell death. A, NAC inhibited DOXO-induced chromatin condensation. HeLa cells infected with 50 m.o.i. of Ad-TIS21 or Ad-β-Gal were exposed to DOXO (1.0 μg/ml) for 12 h with or without NAC (5 mM) pretreatment. The cells with chromatin condensation were counted after Hoechst dye staining. ★, $p < 0.05$ versus Ad-TIS21 infection with DOXO alone. B, Western blot analysis showing inhibition of lamin A/C cleavage by pretreatment with NAC. The data represent the average values with standard deviations and a typical result from three independent experiments.

anti-HA antibody. As shown in Fig. 2B, Ad-TIS21 enhanced DOXO-induced cleavages of PARP and lamin A/C compared with those of the control. However, TIS21 itself did not induce the cleavages when the cells were treated with DOXO. To confirm the pro-apoptotic activity of TIS21 in DOXO-induced cell death, endogenous BTG2^{TIS21} was down-regulated by using sh-BTG2^{TIS21} RNA. Thus, HeLa cells were infected with either lentivirus of BTG2 shRNA (H4 or H5) or empty vector as a control, and the efficiency of knockdown was measured by RT-PCR. As shown in Fig. 2C, RT-PCR revealed down-regulation of BTG2 mRNA in the H4 or H5 infected cells, whereas the expression of glyceraldehyde-3-phosphate dehydrogenase was unaffected. Infection of the cells with sh-BTG2 or control lentiviral vector did not indicate any signs of cell death; however, infection with H4 or H5 significantly reduced the effect of DOXO on the cleavage of lamin A/C (Fig. 2C, right panel). Fig. 2 (A–C) clearly showed pro-apoptotic activity of BTG2 during DOXO-induced cell death in HeLa cells. The findings were unexpected, because BTG2^{-/-} ES cells exhibited increased sensitivity to DOXO-induced cell death (4). To investigate whether the effect of BTG2 on DOXO-induced cell death is not a confined phenomenon in HeLa cells, human hepatocellular carcinoma cell lines Huh7, HepG2, and Hep3B were infected with Ad-TIS21 virus and then treated with IC₅₀ concentrations of DOXO (26) to induce apoptosis. Fig. 2D showed that TIS21 augmented DOXO-induced cleavages of PARP and lamin A/C, compared with those of the Ad-β-Gal. These findings clearly proved the pro-apoptotic role of TIS21 not only in HeLa cells but also in the hepatoma cell lines.

BTG2^{TIS21} Up-regulated Generation of H₂O₂ Induced by DOXO—Based on the report that DOXO produces ROS in cells (27), we first examined whether DOXO was indeed engaged in the apoptotic process of HeLa cells by producing ROS. As expected, ROS in the DOXO-treated HeLa cells was increased as compared with that of the control (Fig. 3A). To further confirm the involvement of ROS in the process, HeLa cells were pretreated with NAC (0–10 mM), a well known H₂O₂ scavenger, and apoptosis was then induced by DOXO. Fig. 3B shows that pretreatment of the cells with NAC-inhibited DOXO-induced cleavage of lamin A/C dose-dependently, indicating that

ROS are indeed involved in cell death. Pretreatment with NAC also led to a dose-dependent decrease in the number of cells with condensed chromatin (data not shown). To investigate the possible involvement of ROS in pro-apoptotic function of BTG2 during DOXO-induced cell death, we first investigated the effect of TIS21^{BTG2} overexpression on superoxide anion generator-induced cell death (28). HeLa cells were incubated with pyrogallol (PYRO; superoxide anion generator), and then NBT reduction by superoxide anion generated was examined. As shown in Fig. 3C, NBT reduction was dependent on

the concentration of PYRO (*upper panel*), and superoxide anion generator-mediated cleavage of PARP was significantly reduced by pretreatment of NAC (*lower panel*), suggesting *in vivo* conversion of PYRO-induced superoxide anion to H₂O₂. When HeLa cells were first infected with 50 m.o.i. of Ad-TIS21 or Ad-β-Gal and then cell death was induced by treatment of the cells with PYRO (50 μM) for 48 h with or without NAC (5 mM) pretreatment, PYRO-induced cell death was enhanced by TIS21, as opposed to inhibition of the enhancement by NAC pretreatment. The finding strongly supports that TIS21 used H₂O₂ to regulate PYRO-induced cell death (Fig. 3D). Thus, employing BTG2 shRNA (H4 and H5) and empty vector as a control (*Con*) we then examined whether the pro-apoptotic effect of BTG2 on DOXO-induced cell death was associated with H₂O₂ generation. As shown in Fig. 3E, DOXO-induced H₂O₂ production was reduced by H4 and H5 infection, as compared with that of the control, indicating up-regulation of H₂O₂ generation by BTG2. To confirm the effect of BTG2^{TIS21} on the generation of intracellular H₂O₂, the cells were infected Ad-TIS21 or Ad-β-Gal viruses, and apoptosis was then induced with DOXO treatment. Treatment of the cells with DOXO significantly increased the level of H₂O₂, and the overexpression of TIS21 further enhanced the H₂O₂ level compared with that of the Ad-β-Gal expression (Fig. 3F). TIS21 itself did not affect the generation of H₂O₂ but significantly enhanced DOXO-induced H₂O₂ generation. Pretreatment of the Ad-TIS21 or Ad-β-Gal-infected cells with NAC inhibited DOXO-induced H₂O₂ generation, indicating that TIS21 up-regulated DOXO-induced H₂O₂ production.

NAC Abolished Effect of BTG2^{TIS21} on DOXO-induced Cell Death—Next, we examined whether the enhanced cell death by BTG2 was regulated by intracellular H₂O₂. Thus, HeLa cells infected with Ad-β-Gal or Ad-TIS21 were exposed to DOXO in the presence of NAC, and cell death was monitored by chromatin condensation. NAC pretreatment abolished the increase of chromatin condensation both in the cells infected with Ad-β-Gal or Ad-TIS21, although Ad-TIS21 infection increased the chromatin condensation more than that of Ad-β-Gal infection (Fig. 4A). Concomitantly, the cleavage of lamin A/C was enhanced after Ad-TIS21 infection, as compared with that of

Pro-apoptotic Activity of BTG2 in Doxorubicin-induced Cancer Cell Death

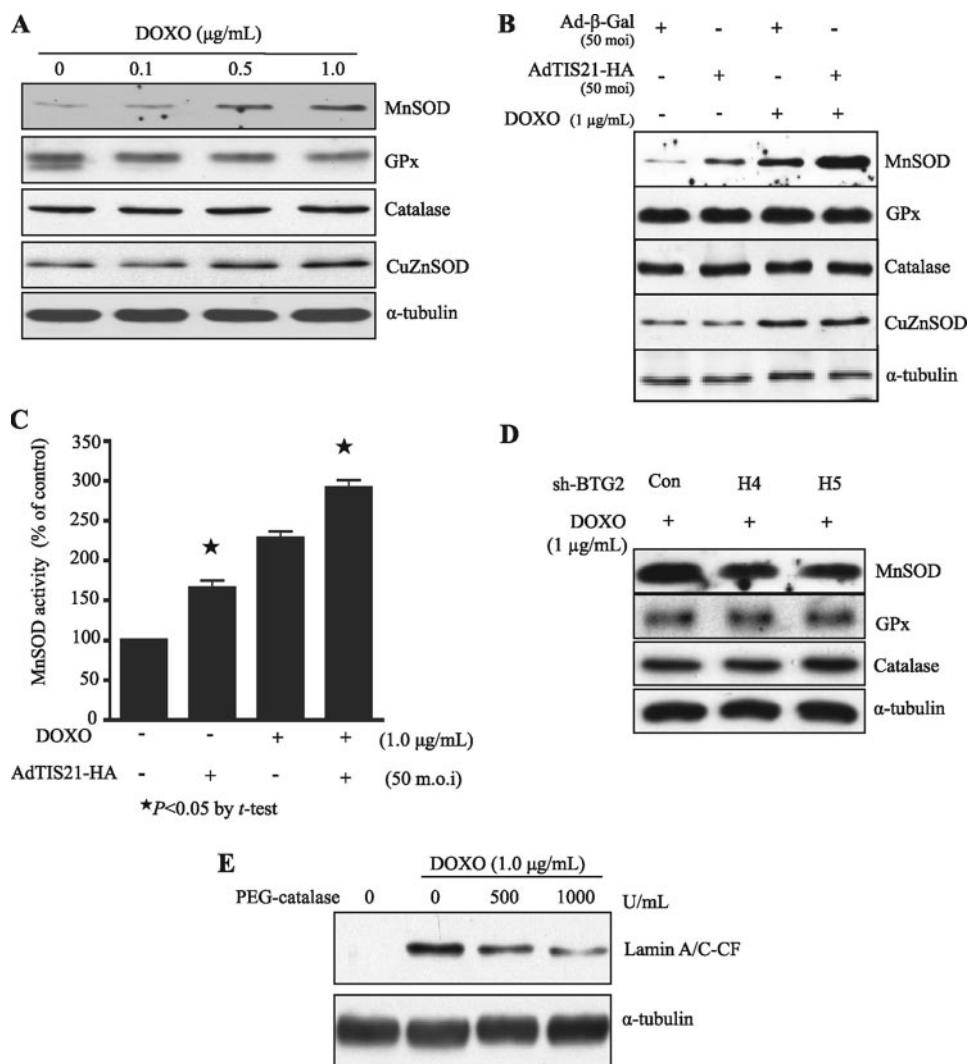


FIGURE 5. BTG2^{TIS21} enhanced expression of MnSOD and its activity, but not other antioxidant enzymes. *A*, Western blot analysis showing the expressions of antioxidant enzymes in HeLa cells treated with the indicated concentrations of DOXO for 12 h. Note the induction of MnSOD and CuZnSOD in response to DOXO treatment, but not GPx and catalase. *B*, Ad-TIS21 enhanced DOXO-induced MnSOD expression without other antioxidant enzymes. In addition to that, Ad-TIS21 alone induced MnSOD, but not CuZnSOD, expression. HeLa cells infected with 50 m.o.i. of Ad-TIS21 or Ad- β -Gal were exposed to DOXO (1.0 $\mu\text{g/mL}$) for 12 h, and then the expressions of antioxidant enzymes were examined by Western blotting. *C*, increase of MnSOD activity by Ad-TIS21 with or without DOXO treatment. HeLa cells were subjected to the analyses of MnSOD activity, after infection with Ad-TIS21 (50 m.o.i.) virus and then with DOXO (1.0 $\mu\text{g/mL}$) for 12 h. Note accordant increase of MnSOD activity with the level of MnSOD expression. *, $p < 0.05$ versus without Ad-TIS21. *D*, inhibition of MnSOD expression by sh-BTG2 infection, but not GPx and catalase. HeLa cells were infected with sh-BTG2 H4 and H5 or empty vector (*Con*) and then treated with DOXO (1.0 $\mu\text{g/mL}$) for 12 h. Expression of antioxidant enzymes was examined by Western blotting. Note inhibition of MnSOD expression in the H4, H5-infected cells. *E*, inhibition of DOXO-induced lamina A/C cleavage by membrane-permeable catalase (PEG-catalase). HeLa cells were pretreated with indicated concentrations of PEG-catalase for 12 h and then treated with DOXO (1.0 $\mu\text{g/mL}$) for 24 h. The cleavage of lamin A/C was determined by Western blotting. Note the inhibition of DOXO-induced cell death by increasing the concentration of PEG-catalase. The data represent a typical result from three independent experiments.

Ad- β -Gal, and NAC pretreatment significantly abolished the effect of Ad-TIS21 (Fig. 4B). The data strongly suggest that H₂O₂ generation may be the major downstream mediator of BTG2^{TIS21} when it works as a pro-apoptotic molecule in DOXO-induced cell death.

BTG2^{TIS21} Up-regulated Expression of MnSOD, but Not Other Antioxidant Enzymes—To investigate a mechanism involved in the significant increase of H₂O₂ in the DOXO-treated HeLa cells, we first examined the effects of DOXO on the expression of antioxidant enzymes. Treatment of HeLa cells

with DOXO (0–1.0 $\mu\text{g/mL}$) for 12 h up-regulated the expression of MnSOD and CuZnSOD in dose-dependent manner, whereas the levels of GPx, catalase, and α -tubulin protein were not changed at all (Fig. 5A), strongly suggesting that the increase of H₂O₂ by DOXO treatment might be due to an imbalance of the coordinated expression of antioxidant enzymes. To investigate whether the up-regulation of MnSOD and CuZnSOD after DOXO treatment was due to the increase of BTG2^{TIS21} in the cells, HeLa cells were infected with Ad-TIS21, and the expression of antioxidant enzymes was measured by Western blot analyses. As shown in Fig. 5B, infection of Ad-TIS21 itself increased MnSOD expression, and TIS21 enhanced the effect of DOXO on the increased expression of MnSOD without any changes of the other enzymes. Although expression of CuZnSOD was also up-regulated by DOXO treatment, the expression was not regulated by TIS21. At the same time, the activity of MnSOD was correlated with its protein level (Fig. 5C). All of the data strongly suggested that the up-regulation of H₂O₂ in the DOXO-treated HeLa cells might result from BTG2^{TIS21}-mediated imbalance of antioxidant enzyme expression. In addition, H4 and H5 sh-BTG2 prevented the effect of TIS21 on the DOXO-induced MnSOD expression (Fig. 5D), indicating that DOXO-induced MnSOD expression might be up-regulated by BTG2^{TIS21}. To verify the hypothesis that the increase of H₂O₂ in the DOXO-treated cells might have been due to an imbalance of the coordinated expressions of antioxidant enzymes, we investigated

whether PEG-catalase, the membrane-permeable form (29), could protect cells from DOXO-induced apoptosis. Thus, HeLa cells were pretreated with PEG-catalase (0–1000 units/ml) for 12 h before DOXO treatment to balance the expression of MnSOD, and DOXO-induced cell death was then examined by immunoblot analysis. PEG-catalase inhibited the cleavage of lamin A/C induced by DOXO treatment (Fig. 5E). These data indicate that BTG2^{TIS21} can augment DOXO-induced cell death via up-regulation of MnSOD, thereby resulting in an imbalance of the coordinated expression of antioxidant

Pro-apoptotic Activity of BTG2 in Doxorubicin-induced Cancer Cell Death

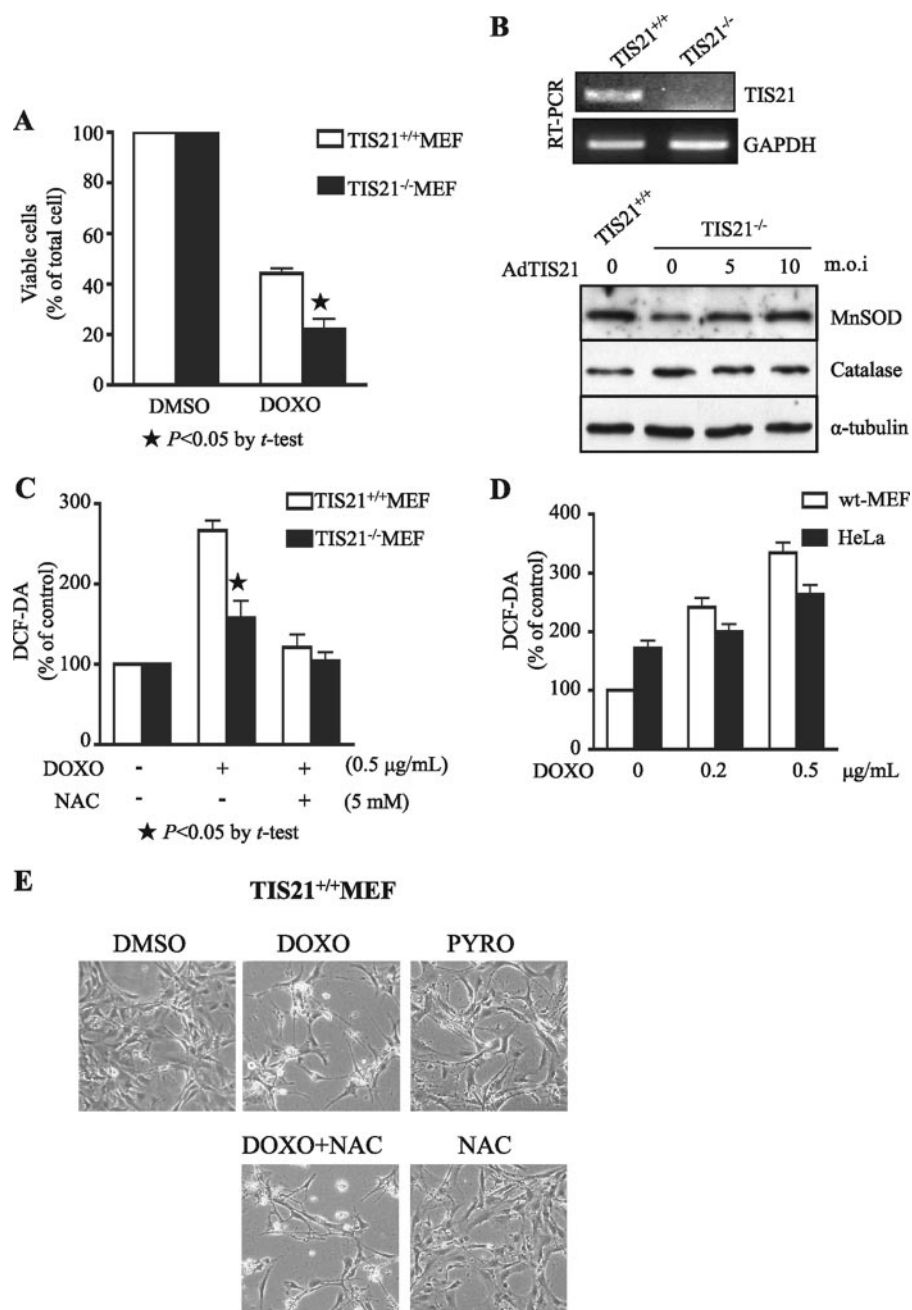


FIGURE 6. Combined treatment with NAC and pyrogallol induced DOXO-induced cell death in MEF cells. A, DOXO-induced cell death was more severe in TIS21^{-/-} MEF than wild type. TIS21^{+/+} MEF and TIS21^{-/-} MEF cells were treated with 0.5 μg/ml of DOXO for 24 h, and then viable cells were determined by trypan blue staining. *, $p < 0.05$ versus DOXO-treated TIS21^{+/+} MEF. B, reconstitution of TIS21 expression in TIS21^{-/-} MEF recovered MnSOD expression. TIS21^{+/+} MEF and TIS21^{-/-} MEF cells were subjected to RT-PCR analysis (upper panel). TIS21^{-/-} MEF cells were infected with indicated concentration of Ad-TIS21 virus for 48 h, and then the cell lysates were subjected to Western blot analyses (lower panel). Note the significant induction of MnSOD expression after Ad-TIS21 infection. C, TIS21 enhanced DOXO-induced H₂O₂ generation in MEF cells. TIS21^{+/+} MEF and TIS21^{-/-} MEF were treated with DOXO (0.5 μg/ml) for 12 h with or without NAC (5 mM) pretreatment. DCFDA fluorescence produced by ROS was measured by flow cytometry. The fluorescence intensity was much stronger in the wild type than the TIS21^{-/-} MEF (*, $p < 0.05$), and NAC further reduced H₂O₂ generation in the MEF cells. D, wild type (wt) MEF and HeLa cells were treated with DOXO (0.5 μg/ml) for 12 h, and DCFDA fluorescence produced by ROS was measured. There was no significant difference of ROS generation between MEF and HeLa cells, supporting the possibility that TIS21 enhanced DOXO-induced H₂O₂ generation in both cells. E, there was no effect of NAC on the DOXO-induced cell death in TIS21^{+/+} MEF cells. When wild type MEF were treated with DOXO (0.5 μg/ml) for 24 h with or without NAC (5 mM) pretreatment, there was no protective effect of NAC against DOXO-induced cell death. Moreover, the cells were resistant to the treatment either with PYRO (100 μM), a superoxide anion and H₂O₂ generator, or NAC, a H₂O₂ scavenger. These data strongly support the concept that cellular response to ROS is quite different based on the cells and cellular context. The photos represent typical and average findings from three repeated experiments.

enzymes with an increase of H₂O₂. Therefore, an increased ratio of MnSOD/catalase appears to enhance DOXO-induced cell death.

No Protective Effect of NAC on DOXO-induced MEF Cell Death—Although the present findings indicate that BTG2 augments DOXO-induced cell death in HeLa cells, BTG2^{PC3/TIS21} knock-out ES cells were known to be more sensitive to DOXO-induced cell death compared with wild type (4). To confirm the role of BTG2 in DOXO-induced cell death in ES cells, we employed our TIS21^{-/-} MEF (24, 30, 31). As opposed to TIS21^{+/+} MEF, exposure of TIS21^{-/-} MEF to DOXO demonstrated a lower number of viable cells, suggesting the anti-apoptotic role of TIS21 gene in MEF (Fig. 6A). To investigate whether the anti-apoptotic effect of BTG2 was related to antioxidant enzymes, expressions of MnSOD and catalase were examined in the TIS21^{-/-} MEF (Fig. 6B). MnSOD, but not catalase, expression was lower in the TIS21^{-/-} MEF than that of wild type MEF. Moreover, reconstitution of TIS21 gene by infection of TIS21^{-/-} MEF with Ad-TIS21 virus, MnSOD, but not catalase, expression was regulated according to the level of Ad-TIS21 (0–10 m.o.i.). The phenomenon was in close accordance with our previous data (Fig. 5, B–D) that TIS21 itself up-regulated MnSOD expression and its activity. When the effect of TIS21 on ROS was evaluated, treatment of wild type MEF with DOXO generated more H₂O₂ than that of TIS21^{-/-} MEF (Fig. 6C). However, it was significantly reduced by NAC pretreatment. When we compared the generation of H₂O₂ after DOXO treatment, the amount of H₂O₂ generated in wild type MEF was not lower than that of HeLa cells (Fig. 6D). These findings indicate that although TIS21 exhibited pro-apoptotic and anti-apoptotic activities in HeLa and MEF, respectively, TIS21 enhanced H₂O₂ generation in response to DOXO treatment both in HeLa and MEF cells via regulation of MnSOD.

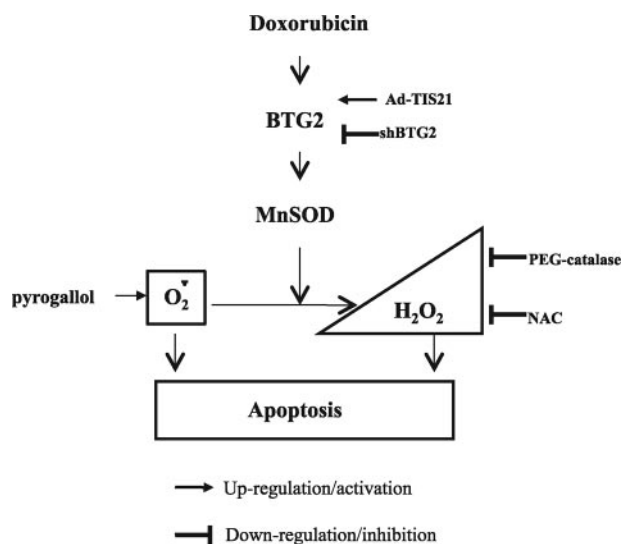


FIGURE 7. Schema showing the pro-apoptotic role of BTG2^{TIS21} in DOXO-induced cell death. Treatment of HeLa cells with DOXO increased expressions of BTG2 and MnSOD, without any other antioxidant enzymes. Expression and activity of MnSOD were accordingly regulated by TIS21 gene, evaluated by infection of cancer cells with Ad-TIS21 or sh-BTG2 viruses. Moreover, TIS21 enhanced ROS generation induced by DOXO or pyrogallol both in cancer cells and MEF, which was further confirmed by pretreatment with NAC, a H₂O₂ scavenger. Therefore, H₂O₂ accumulation caused by the increased MnSOD resulted in cancer cell death, whereas it was alleviated by membrane-permeable catalase (PEG-catalase) as well as NAC treatment. On the other hand, MEF responded differently to H₂O₂ produced by DOXO or pyrogallol treatment and further enhanced by TIS21 expression. In summary, TIS21 works as an enhancer of chemotherapeutic agent by accumulating H₂O₂ in cancer cells via induction of MnSOD expression and its activity, which leads to an imbalance of the antioxidant system.

To further characterize role of H₂O₂ in normal cells, we next examined the effect of oxidative stress in the DOXO-induced MEF cell death. In contrast to the protective role of NAC in DOXO-induced HeLa cell death (Fig. 3B), pretreatment of MEF with NAC failed to block DOXO-induced MEF cell death (Fig. 6E). Moreover, treatment of MEF with either NAC, H₂O₂ scavenger, or 100 μM pyrogallol (PYRO), a specific generator of superoxide anion and H₂O₂, revealed no phenotypical differences, particularly in cell death, as compared with DMSO treatment. These findings strongly suggest that ROS may not play a pro-apoptotic role in MEF, although TIS21^{BTG2} enhanced DOXO-induced H₂O₂ generation both in HeLa and MEF cells. In summary, BTG2^{TIS21} worked as an enhancer of DOXO-induced cell death in HeLa, but anti-apoptotic in MEF.

DISCUSSION

We demonstrated here that induction of BTG2^{TIS21/PC3} expression sensitized HeLa cells to DOXO-mediated cell death via imbalance of antioxidant enzyme, e.g. induction of MnSOD, but not catalase and GPx, thereby resulting in H₂O₂ generation (Fig. 7). The phenomenon was confirmed by infections of Ad-TIS21 virus and lentivirus carrying sh-BTG2 RNA, in addition to treatments of NAC and membrane-permeable catalase. The mechanism of significant induction of BTG2^{TIS21/PC3} expression after DOXO treatment (Fig. 1C) could be well supported by the presence of four tandem PuPuPuC(A/T) pentamer, a potential p53 recognition element (32), on the 5'-untranslated region of BTG2 gene (4). DOXO-induced BTG2 expression has

been known to be p53-dependent in MCF-7 cells (33), whereas 12-O-tetradecanoylphorbol-13-acetate induces BTG2 expression in U937 cells p53-independently (10). Furthermore, infection of HeLa cells with Ad-TIS21 virus significantly enhanced DOXO-induced HeLa cell death (Fig. 2, A and B), whereas sh-BTG2 RNA in lentivirus reduced apoptosis (Fig. 2C), strongly supporting a pro-apoptotic role for BTG2^{TIS21/PC3} in cancer cells, not only HeLa cells but also Huh7, HepG2, and Hep3B cells (Fig. 2D).

It has been known that DOXO induces ROS generation by utilizing cellular oxidoreductases (34, 35), such as NADH dehydrogenase complex, NADPH cytochrome p450 reductase (36), and xanthine oxidase, as well as by nonenzymatic pathways via complex formation between DOXO-ferric iron (37); electron donor activates benzantraquinones of DOXO to semiquinones, and a single electron is transferred to molecular oxygen, thereby generating free radicals, such as superoxide anion, H₂O₂, hydroxyl radical, and other reactive nitrogen-species (38). Indeed, treatment of HeLa cells with DOXO generated ROS (Fig. 3A), and DOXO-induced H₂O₂ generation was significantly regulated by TIS21 expression, e.g. increased by Ad-TIS21 infection (Fig. 3E) but decreased by sh-BTG2^{TIS21} RNA and NAC treatment (Fig. 3F). Oxidative damage, therefore, has long been considered to be an important mechanism of anthracycline activity in tumor cells (27). In the present study, DOXO-induced chromatin condensation and cleavage of lamin A/C were aggravated by introduction of TIS21 to HeLa cells, however, pretreatment of the cells with NAC significantly reduced the damage by DOXO (Fig. 4), supporting the idea that TIS21 works as a pro-apoptotic molecule by enhancing ROS generation upon the treatment of cancer cells with DOXO. When we employed PYRO, TIS21 also enhanced PYRO-induced HeLa cell death; however, it was completely blocked by NAC pretreatment (Fig. 3D). The data strongly suggest that TIS21 enhanced PYRO-induced superoxide and its conversion to H₂O₂.

In addition to ROS generation, MnSOD has recently been identified as a potential target of p53, and ROS have been identified as downstream mediators of tumor suppressor p53 (39). Therefore, it is rather tempting to postulate that DOXO induces p53 activation and BTG2^{TIS21/PC3} expression, which in turn up-regulates ROS generation and enhances cell death. Indeed, infection of HeLa cells with Ad-TIS21 itself up-regulated MnSOD expression before DOXO treatment, and the expression of MnSOD, but not catalase, GPx, and CuZnSOD, was additively increased after DOXO treatment caused by endogenous BTG2 and exogenous TIS21 activities (Fig. 5, B and C). Thus, a question arises of why high induction of MnSOD enhanced DOXO-induced cell death. Even though the role of SOD as an antioxidant defense has been extensively documented, high activities of SOD have sometimes been reported to be toxic *in vivo* (40); therefore the higher the level of SOD, the greater the rate of accumulation of H₂O₂ (41). Furthermore, up-regulation of MnSOD has been shown to induce and inhibit apoptotic effects of c-Rel in the same cells (42, 43).

In this study, we presented pro-apoptotic role of BTG2 in the DOXO-induced cancer cell death. However, that is in conflict with a previous report regarding the anti-apoptotic effect of

Pro-apoptotic Activity of BTG2 in Doxorubicin-induced Cancer Cell Death

BTG2^{PC3/TIS21} in ES cells (4). We therefore employed TIS21^{-/-} MEF and confirmed that TIS21 enhanced DOXO-induced H₂O₂ generation not only in cancer cells but also in MEF; however, the cellular response to H₂O₂ was quite different between cancer and normal cells (Fig. 6). This conflict can be well supported by the report that the effect of ROS in cells is quite different based on the cellular context; mitogenic response, growth arrest, senescence, and cell death (44). We cannot presently explain why H₂O₂ produced by TIS21 shows such a different effect on cell death between cancer cells and embryonic cells. However, as far as we know, this is the first report to show that BTG2 enhances DOXO-induced cancer cell death via up-regulation of MnSOD. Therefore, we suggest that BTG2^{TIS21/PC3} augments DOXO-induced cancer cell death via deregulation of antioxidant enzymes, resulting in increased susceptibility to DOXO-induced oxidative damage.

REFERENCES

1. Lim, R. W., Varnum, B. C., and Herschman, H. R. (1987) *Oncogene* **1**, 263–270
2. Fletcher, B. S., Lim, R. W., Varnum, B. C., Kujubu, D. A., Koski, R. A., and Herschman, H. R. (1991) *J. Biol. Chem.* **266**, 14511–14518
3. Bradbury, A., Possenti, R., Shooter, E. M., and Tirone, F. (1991) *Proc. Natl. Acad. Sci. U. S. A.* **88**, 3353–3357
4. Rouault, J. P., Falette, N., Guehenneux, F., Guillot, C., Rimokh, R., Wang, Q., Berthet, C., Moyret-Lalle, C., Savatier, P., Pain, B., Shaw, P., Berger, R., Samarut, J., Magaud, J. P., Ozturk, M., Samarut, C., and Puisieux, A. (1996) *Nat. Genet.* **14**, 482–486
5. Lim, I. K., Lee, M. S., Lee, S. H., Kim, N. K., Jou, I., Seo, J. S., and Park, S. C. (1995) *J. Cancer Res. Clin. Oncol.* **121**, 279–284
6. Struckmann, K., Schraml, P., Simon, R., Elmenhorst, K., Mirlacher, M., Kononen, J., and Moch, H. (2004) *Cancer Res.* **64**, 1632–1638
7. Ficazzola, M. A., Fraiman, M., Gitlin, J., Woo, K., Melamed, J., Rubin, M. A., and Walden, P. D. (2001) *Carcinogenesis* **22**, 1271–1279
8. Boiko, A. D., Porteous, S., Razorenova, O. V., Krivokrysenko, V. I., Williams, B. R., and Gudkov, A. V. (2006) *Genes Dev.* **20**, 236–252
9. Lim, I. K., Lee, M. S., Ryu, M. S., Park, T. J., Fujiki, H., Eguchi, H., and Paik, W. K. (1998) *Mol. Carcinog.* **23**, 25–35
10. Ryu, M. S., Lee, M. S., Hong, J. W., Hahn, T. R., Moon, E., and Lim, I. K. (2004) *Exp. Cell Res.* **299**, 159–170
11. Hong, J. W., Ryu, M. S., and Lim, I. K. (2005) *J. Biol. Chem.* **280**, 21256–21263
12. Fridovich, I. (1995) *Annu. Rev. Biochem.* **64**, 97–112
13. Zelko, I. N., Mariani, T. J., and Folz, R. J. (2002) *Free Radic. Biol. Med.* **33**, 337–349
14. Li, Y., Huang, T. T., Carlson, E. J., Melov, S., Ursell, P. C., Olson, J. L., Noble, L. J., Yoshimura, M. P., Berger, C., Chan, P. H., Wallace, D. C., and Epstein, C. J. (1995) *Nat. Genet.* **11**, 376–381
15. Scott, M. D., Meshnick, S. R., and Eaton, J. W. (1987) *J. Biol. Chem.* **262**, 3640–3645
16. Scott, M. D., Meshnick, S. R., and Eaton, J. W. (1989) *J. Biol. Chem.* **264**, 2498–2501
17. Li, N., Oberley, T. D., Oberley, L. W., and Zhong, W. (1998) *Prostate* **35**, 221–233
18. Chen, J. G., Yang, C. P., Cammer, M., and Horwitz, S. B. (2003) *Cancer Res.* **63**, 7891–7899
19. Islaih, M., Halstead, B. W., Kadura, I. A., Li, B., Reid-Hubbard, J. L., Flick, L., Altizer, J. L., Thom Deahl, J., Monteith, D. K., Newton, R. K., and Watson, D. E. (2005) *Mutat. Res.* **578**, 100–116
20. Tirone, F. (2001) *J. Cell Physiol.* **187**, 155–165
21. Lee, Y., and Shacter, E. (1997) *Blood* **89**, 4480–4492
22. Kim, H. S., Song, M. C., Kwak, I. H., Park, T. J., and Lim, I. K. (2003) *J. Biol. Chem.* **278**, 37497–37510
23. Serrander, L., Cartier, L., Bedard, K., Banfi, B., Lardy, B., Plastre, O., Sienkiewicz, A., Fórró, L., Schlegel, W., and Krause, K. (2007) *Biochem. J.* **406**, 105
24. Park, T. J., Kim, J. Y., Oh, S. P., Kang, S. Y., Kim, B. W., Wang, H. J., Song, K. Y., Kim, H. C., and Lim, I. K. (2008) *Hepatology* **47**, 1533–1543
25. Zaleskis, G., Berleth, E., Verstovsek, S., Ehrke, M. J., and Mihich, E. (1994) *Mol. Pharmacol.* **46**, 901–908
26. Lee, T. K., Lau, T. C., and Ng, I. O. (2002) *Cancer Chemother. Pharmacol.* **49**, 78–86
27. Minotti, G., Menna, P., Salvatorelli, E., Cairo, G., and Gianni, L. (2004) *Pharmacol. Rev.* **56**, 185–229
28. Kim, S. W., Han, Y. W., Lee, S. T., Jeong, H. J., Kim, S. H., Kim, I. H., Lee, S. O., Kim, D. G., Kim, S. Z., and Park, W. H. (2008) *Mol. Carcinog.* **47**, 114–125
29. Beckman, J. S., Minor, R. L., Jr., White, C. W., Repine, J. E., Rosen, G. M., and Freeman, B. A. (1988) *J. Biol. Chem.* **263**, 6884–6892
30. Park, S., Lee, Y. J., Lee, H. J., Seki, T., Hong, K. H., Park, J., Beppu, H., Lim, I. K., Yoon, J. W., Li, E., Kim, S. J., and Oh, S. P. (2004) *Mol. Cell Biol.* **24**, 10256–10262
31. Kim, B. C., Ryu, M. S., Oh, S. P., and Lim, I. K. (2008) *Stem Cells* **26**, 2339–2348
32. el-Deiry, W. S., Kern, S. E., Pietenpol, J. A., Kinzler, K. W., and Vogelstein, B. (1992) *Nat. Genet.* **1**, 45–49
33. Cortes, U., Moyret-Lalle, C., Falette, N., Duriez, C., Ghissassi, F. E., Barnas, C., Morel, A. P., Hainaut, P., Magaud, J. P., and Puisieux, A. (2000) *Mol. Carcinog.* **27**, 57–64
34. Vasquez-Vivar, J., Martasek, P., Hogg, N., Masters, B. S., Pritchard, K. A., Jr., and Kalyanaraman, B. (1997) *Biochemistry* **36**, 11293–11297
35. Minotti, G., Cairo, G., and Monti, E. (1999) *FASEB J.* **13**, 199–212
36. Bachur, N. R., Gordon, S. L., Gee, M. V., and Kon, H. (1979) *Proc. Natl. Acad. Sci. U. S. A.* **76**, 954–957
37. Eliot, H., Gianni, L., and Myers, C. (1984) *Biochemistry* **23**, 928–936
38. Tokarska-Schlattner, M., Zaugg, M., Zuppinger, C., Wallimann, T., and Schlattner, U. (2006) *J. Mol. Cell Cardiol.* **41**, 389–405
39. Pani, G., Bedogni, B., Anzevino, R., Colavitti, R., Palazzotti, B., Borrello, S., and Galeotti, T. (2000) *Cancer Res.* **60**, 4654–4660
40. Gardner, R., Salvador, A., and Moradas-Ferreira, P. (2002) *Free Radic. Biol. Med.* **32**, 1351–1357
41. Buettner, G. R., Ng, C. F., Wang, M., Rodgers, V. G., and Schafer, F. Q. (2006) *Free Radic. Biol. Med.* **41**, 1338–1350
42. Bernard, D., Quatannens, B., Begue, A., Vandenbunder, B., and Abbadie, C. (2001) *Cancer Res.* **61**, 2656–2664
43. Bernard, D., Monte, D., Vandenbunder, B., and Abbadie, C. (2002) *Oncogene* **21**, 4392–4402
44. Martindale, J. L., and Holbrook, N. J. (2002) *J. Cell Physiol.* **192**, 1–15